Prediction and Measurement of the local extinction coefficient in sprays for 3D simulation/experiment data comparison

CrossMark

H. Grosshans [a,*], E. Kristensson [b], R.-Z. Szász [c], E. Berrocal [b,*]

[a] Interdisciplinary Center for Scientific Computing (IWR), University of Heidelberg, 69120 Heidelberg, Germany
[b] Division of Combustion Physics, Lund University, Box 118, 22100 Lund, Sweden
[c] Division of Fluid Mechanics, Lund University, Box 118, 22100 Lund, Sweden

ABSTRACT

In the recent years, large progresses in laser imaging techniques have allowed to extract spatially resolved 2D and 3D quantitative spray information even in optically dense situations. The main breakthrough of these techniques is the possibility of suppressing unwanted effects from multiple light scattering using Structured Illumination. Thanks to this new feature, effects due to light extinction can also be corrected allowing the measurement of the local extinction coefficient. These quantitative information which is available even in challenging conditions, where Phase Doppler does not work anymore, can be used for data comparison between experiment and simulation. The local extinction coefficient is particularly valuable for the description of the droplet field, defined as the "*spray region*", as it contains information related to both droplets size and concentration. In this article we detail, then, the procedure enabling the modelers to obtain numerically this local extinction coefficient over the full 3D spray system. Following this procedure, results can now be adequately compared between simulation and experiment. The proposed comparison approach can better guide model adjustments in situation where the initial droplet size distribution is unknown or approximated and presents a step towards future validations of spray simulations, especially those based on Lagrangian Particle Tracking. The approach is exemplified here for the case of a Diesel-type spray. The results reveal at which specific spray locations discrepancies occur, and highlight the sensitivity of the initial droplet size distribution on the resulting extinction coefficient.

Introduction

A numerical model capable of simulating faithfully the process of liquid atomization and droplet transport, would permit the three-dimensional prediction of the droplet size distribution, number density, velocity and evaporation rate over time. Such predictions could considerably help for the further development and optimization of industrial devices such as liquid fuel driven combustion engines or spray dryers. On the contrary, spray simulation results from a model that is partly or not validated are of very limited importance as they cannot be used as a reliable tool for the study of spray formation at various initial conditions. It is, thus, of utmost importance to fully validate spray simulations, a process that includes both the use of trustable experimental data as well as the development of adequate comparison procedures.

As discussed in past review articles (Loth, 2000; van Wachem and Almstedt, 2003; Balachandar and Eaton, 2010) the numerical approaches used to describe dispersed liquid–gas flows can be grouped as One-fluid, Two-fluid, Lagrangian Particle Tracking, Interface Resolving (e.g. Volume of Fluid, level-set) and Lattice-Boltzmann approaches. The first two approaches are usually limited to certain flow types such as, for instance, limited Stokes number ranges or monodisperse sprays. On the opposite, the latter two methods can be very accurate in any flow conditions if an adequate fine grid is employed. Therefore, they are usually applied to describe the so-called "*spray formation region*" (Linne, 2013) (see illustration in Fig. 1) where primary breakups occurs (Shinjo and Umemura, 2011; Menard et al., 2006; Desjardins et al., 2008). Even though accurate, those simulations are, however, highly demanding in terms of calculation effort and cannot, yet, be applied for the case of a large spray system which includes numerous liquid structures of various sizes. Finally, the Lagrangian

* Corresponding authors.
E-mail addresses: holger.grosshans@iwr.uni-heidelberg.de (H. Grosshans), edouard.berrocal@forbrf.lth.se (E. Berrocal).

Particle Tracking (LPT) (Dukowicz, 1980) presents a good compromise as it is more accurate than the One-fluid and Two-fluid methods and at the same time it is not too much computer demanding when the entire "*spray region*" (see illustration in Fig. 1) needs to be simulated. For these reasons, and due to its flexibility, the LPT approach is particularly attractive and popular for the simulation of the spray region where droplets transport, secondary break-up and droplet evaporation occur.

In terms of experiment, the validation of models describing the spray formation region requires the recordings of high resolution and high contrast images in order to visualize spray dynamics from the near-nozzle region. The laser imaging techniques which are most suitable for this task are Ballistic Imaging (Linne et al., 2009), Single-shot SLIPI (Kristensson et al., 2010, 2014) and high resolution microscopic imaging (Crua et al., 2012). However, for the validation of numerical models describing the spray region, a statistical description of the spray over a large field-of-view is required. In this case, averaged imaging can be employed together with, if possible, a 3-D image reconstruction scheme. The most adequate laser imaging techniques for this task are based on the use of Structured Illumination (e.g. SLIPI scan, Tomo-SLITI and Dual SLIPI, highlighted in blue in Fig. 1). This article is introducing these techniques to the reader. Based on the use of those techniques, the presented work aims at providing answers to the following questions:

- Which quantity can possibly be measured in two- or three-dimension with high spatial resolution through the spray region in optically dense situations?
- How can this quantity be numerically extracted in order to be compared with the experimental data?

In this article the proposed quantity is the so-called local extinction coefficient: The extinction coefficient μ_e (in mm^{-1}), also referred in the literature as attenuation coefficient, is an optical property equal to the product of the droplet concentration N and the droplets extinction cross-section σ_e; where σ_e can be seen as an hypothetical area which describes the likelihood of light to interact with a droplet through scattering or absorption. It is a quantity used to describe the optical density of a medium which can be extracted by measuring the attenuation of a beam crossing a scattering/absorbing medium like a spray system.

Using recent laser imaging techniques based on Structured Illumination (see Fig. 1), it has been demonstrated that μ_e can be extracted locally in a spray providing 2D and 3D resolved data, even in optically dense situations. This set of data which was not available in the past, due to effects of multiple light scattering, can now be used for experiment/simulation comparison purposes. It should be noted that such experimental results would not directly validate a model (as the extinction coefficient contains information of both droplets size and concentration), but they do indicate whether the modeling results are incorrect. In addition, this comparison based on a field variable provides further insights of the spray structure than when based on global spray parameters only.

It is of importance to emphasize to spray modelers the availability of this new type of data. The second thing of equal importance is to provide modelers, who might not be familiar with the concept of local extinction coefficient, with the procedure to adequately extract it for reliable comparison with recent experimental data. Such an approach, proposed in this article, presents a first step towards the validation of models for the analysis of the spray region in optically dense situations. The procedure is exemplified here for the case of a Diesel spray.

How to compare simulated and experimental data from the spray region in optically dense situations?

Description of previous comparison approaches

The droplet size distribution, concentration and velocity have been, naturally, considered as validation parameters (Broukal and Hajek, 2011). Those data are most often experimentally measured using Phase Doppler Anemometry (PDA) due to the good accuracy, robustness, large dynamic range and availability of commercial instruments. In addition, droplet size-velocity correlations can be derived from PDA data which is of great interest for model validation purposes.

However, despite its large merits, Phase Doppler remains a point measurement technique strongly restricting the possibility of two- and three-dimensional measurements. Furthermore, the technique is time averaged and most importantly, it is not applicable for optically dense situations.

As a consequence to the lack of accessible quantitative data, the global structure and geometrical characteristics of atomizing sprays have instead been used extensively for comparison purposes e.g. in Faeth et al. (1995), Naber and Siebers (1996), Martínez-Martínez et al. (2008) or Wu et al. (2006). This includes comparative analyses of the spray penetration length, the vapor penetration distance and the spray opening angle which have been performed from the earliest years of spray simulation validations until today (Dukowicz, 1980; Beck and Watkins, 2002; Apte et al., 2003; Andreassi et al., 2007; Fu-shui et al., 2008; Shim et al., 2009).

However, trying to validate a model based on those global parameters involves several drawbacks. First, spray simulations contain large number of input parameters that can be tuned to intentionally meet the global spray parameters measured experimentally. Thus, it should be no surprise that the simulated spray penetration length and the spray angle can both agree well with those measured experimentally. Second, even if two sprays show the same global parameters, their internal structure can still be significantly different one from another. Third, the definitions of those global parameters are often inconsistent. One typical example is the estimation of the spray penetration length. The usual experimental method to measure it is to fix a threshold value relative to the maximum of light intensity detected by the camera. However, this approach suffers from a number of issues:

1. The illumination light intensity profile differs both temporally and spatially from one measurement to another.
2. Cameras vary in sensitivity, dynamic range and detection response at different wavelengths.
3. Different scattering processes (e.g. Mie scattering or fluorescence) lead to a different visualization of the spray (see Fig. 2).
4. Blurring effects induced from multiple light scattering smooth out structural details of the spray.

As a result of these combined effects, the spray penetration length would be estimated differently by different research groups, even though the operating conditions are exactly the same and even though the acquired data is post-processed equally. Fig. 2 illustrates this issue where a Diesel spray is imaged simultaneously using planar Mie scattering and liquid Laser Induced Fluorescence (LIF). Here a threshold value at 5% of the maximum intensity is used to deduce the contours of the spray. Even though simultaneously acquired with two identical cameras, the spray penetration length is shorter in the LIF images than in the corresponding Mie cases. Furthermore, the shape of the spray does not agree neither. In this example the observed discrepancies are explained by the
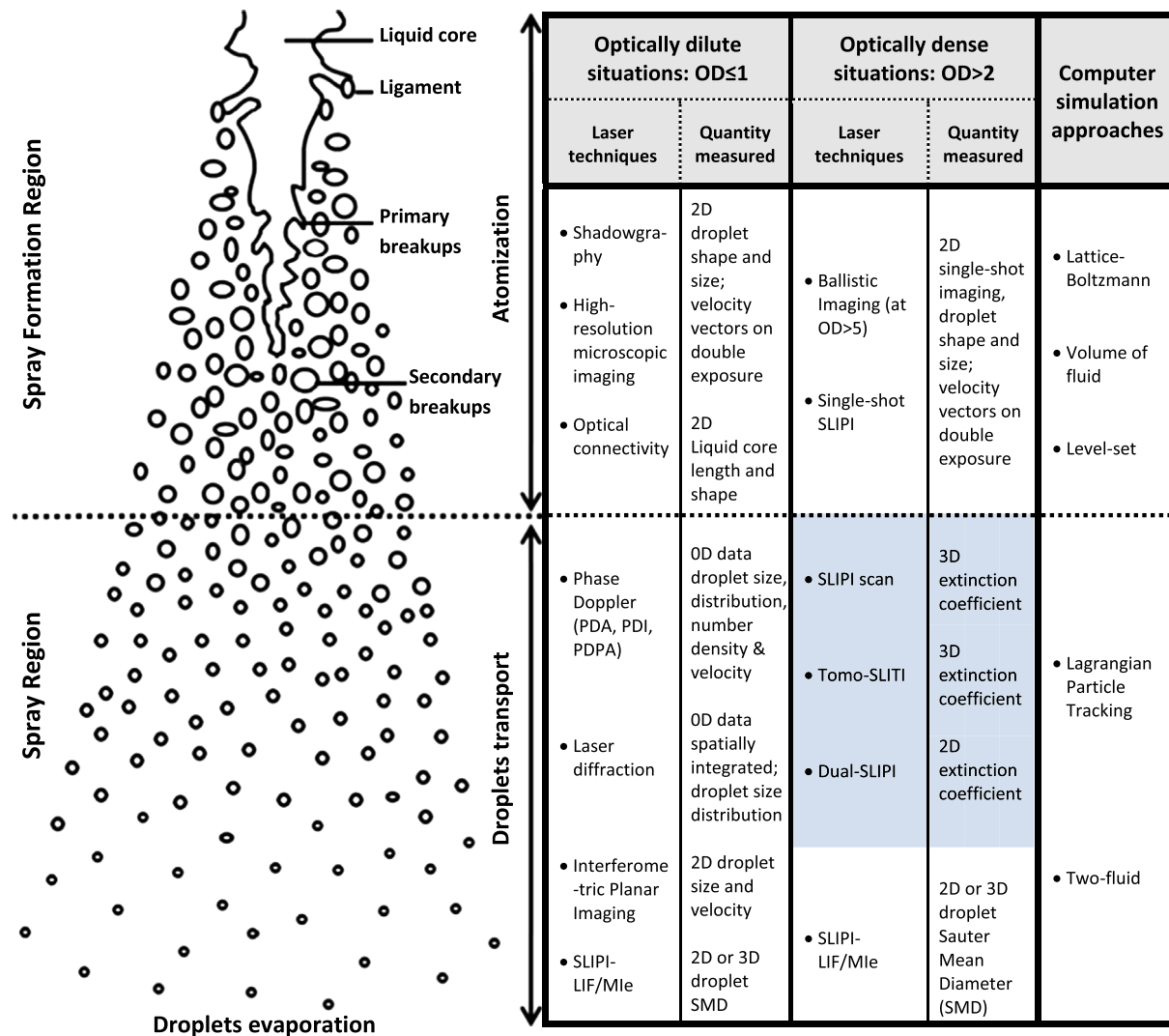
	Optically dilute situations: OD≤1		Optically dense situations: OD>2		Computer simulation approaches
	Laser techniques	Quantity measured	Laser techniques	Quantity measured	
Atomization	• Shadowgraphy • High-resolution microscopic imaging • Optical connectivity	2D droplet shape and size; velocity vectors on double exposure 2D Liquid core length and shape	• Ballistic Imaging (at OD>5) • Single-shot SLIPI	2D single-shot imaging, droplet shape and size; velocity vectors on double exposure	• Lattice-Boltzmann • Volume of fluid • Level-set
Droplets transport	• Phase Doppler (PDA, PDI, PDPA) • Laser diffraction • Interferometric Planar Imaging • SLIPI-LIF/Mie	0D data droplet size, distribution, number density & velocity 0D data spatially integrated; droplet size distribution 2D droplet size and velocity 2D or 3D droplet SMD	• SLIPI scan • Tomo-SLITI • Dual-SLIPI • SLIPI-LIF/Mie	3D extinction coefficient 3D extinction coefficient 2D extinction coefficient 2D or 3D droplet Sauter Mean Diameter (SMD)	• Lagrangian Particle Tracking • Two-fluid

Diagram labels: Liquid core; Ligament; Primary breakups; Secondary breakups; Spray Formation Region; Spray Region; Atomization; Droplets transport; Droplets evaporation.

Fig. 1. Characteristics of atomizing sprays showing both the spray formation region and the spray region. For each region, a categorization of both the experimental laser techniques and of the simulation approaches usually applied is shown. The experimental techniques are divided into two categories corresponding to optically dense and optically dilute situations. In optically dense situations the effects from multiple light scattering must be suppressed. The Structured Illumination based techniques, highlighted in blue, present an interesting possibility to extract up to 3D data from the spray region even in optically dense situations. (For interpretation of the references to colour in this figure legend, the reader is referred to the web version of this article.)

fact that the Mie and the LIF signal are respectively related to the surface area and the volume of the droplets. Cameras with different dynamic ranges and sensitivities would lead to similar effects. This illustrates the uncertainty associated with the spray penetration length when based on the recording of light intensity values and the inadequacy of using such data for model comparison purposes.

Recently, Picket et al. (2011) have investigated those effects and concluded that light extinction measurements were the most reliable for providing an improved assessment of the physical meaning of liquid-length measurements in Diesel spray. Instead of measuring the extinction coefficient along the beam path (0D data), we are proposing, in this article, to measure it locally in order to obtain spatially resolved 3D data.

A novel comparison approach using the local extinction coefficient

In this paper we propose to use a quantity known as the local light extinction coefficient, μ_e, for a comparison between experiment and simulation regarding the spray region. The extinction coefficient is an optical quantity (wavelength dependent)

containing information related to both the droplet size and number density. It can be experimentally extracted only if the measurement is not affected by effects introduced by multiple light scattering. This is the case when the spray is either optically dilute or if the intensity contribution from multiple light scattering is efficiently suppressed. The spray region is defined as optically dilute when the light transmission $I(x)/I(0)$ is >37%. Under such conditions, the average number of interactions between photons and droplets along the incident laser beam path is inferior than one making the single scattering approximation valid. At light transmission lower than 37% photons interact statistically more than once with the surrounding droplets inducing multiple light scattering effects.

Experimentally, μ_e is a quantity that is directly measurable from spray systems illuminated with a monochromatic and collimated source of light, such as a laser beam. It describes the rate at which the beam loses its irradiance I over the distance x, while crossing a homogeneous scattering and/or absorbing medium, such as a spray. This intensity loss is mathematically related to the extinction coefficient as
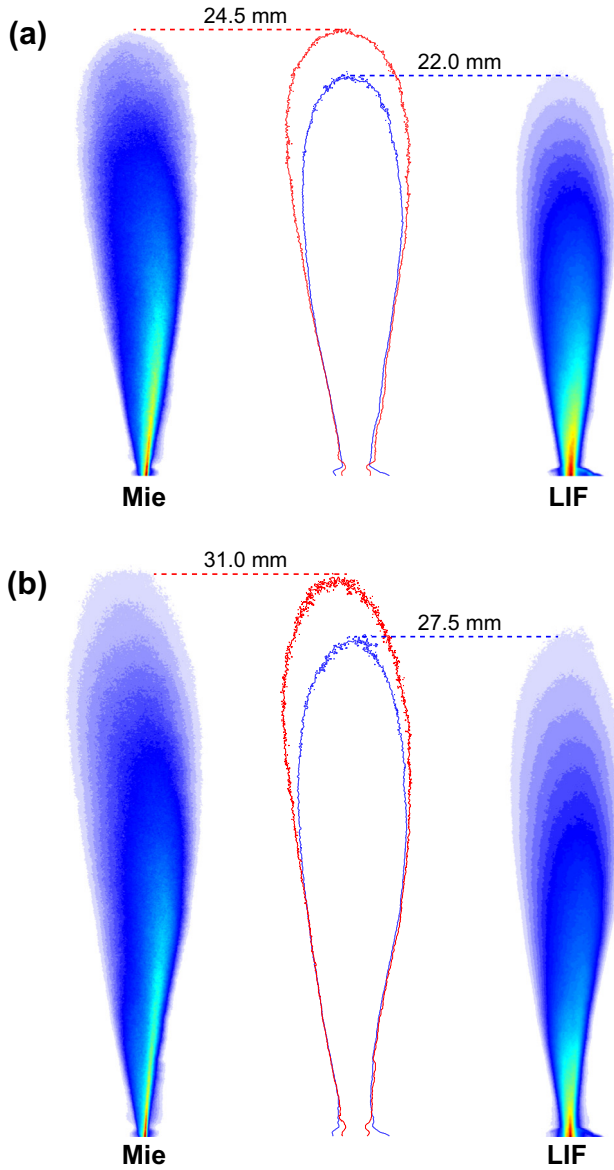
$$dI = -\mu_e \cdot I \cdot dx. \tag{1}$$

Fig. 2. Illustration of the disagreements in the experimental determination of the spray penetration length between LIF and Mie detection (Berrocal et al., 2012, data taken from). Here a threshold at 5% of the maximum intensity is used for (a) $t = 500\,\mu s$ and (b) $t = 750\,\mu s$ after injection starts. Even though the images have been recorded simultaneously, the estimation of the spray penetration length shows clear discrepancies between the liquid LIF and the Mie scattering signals. Similar discrepancies are likely to occur for images recorded with different cameras and illumination sources.

The solution to Eq. (1) is the well-known Beer–Lambert law, stating that the light intensity reduces exponentially as it propagates through a scattering and/or absorbing medium,

$$I(x) = I(0) \cdot \exp(-\mu_e \cdot x) = I(0) \cdot \exp(-OD), \qquad (2)$$

where OD is referred to as the optical depth of the medium, also denoted in literature as τ. The inverse of the extinction coefficient defines the photon mean free path $l_{fpl} = 1/\mu_e$ which is the average distance between two photons/droplet interactions. If a laser beam crosses a distance x in a spray, the division x/l_{fpl} equals to the average number of scattering events along the laser beam path. As a result, $x/l_{fpl} = \mu_e \cdot x = OD$, meaning that the optical depth corresponds to the average number of scattering events along the length crossed by an incident beam. When $OD = 1$, corresponding to the single light scattering regime, the light transmission $I(x)/I(0)$ equals

37%. In the case of the spray region, μ_e depends only on the droplet concentration N and the droplets extinction cross-section σ_e. If a monodisperse cloud of droplets is illuminated at a single wavelength, μ_e can be estimated as

$$\mu_e = \sigma_e \cdot N. \qquad (3)$$

The extinction cross-section σ_e relates to the effective area of droplet/light interaction and is directly related to the droplets size. The extinction cross-section equals the sum of the scattering and the absorption cross-sections ($\sigma_e = \sigma_s + \sigma_a$). If the droplets are non-absorbing at the illumination wavelength then only scattering occurs and the extinction cross-section equals the scattering cross-section. A detailed description of the extinction cross-section and how to deduce it in the case of spherical droplets is given in Section 'Determination of the extinction cross-sections'.

By using the local extinction coefficient as the parameter of comparison a complete field of a variable can be used instead of global parameters and qualitative spray descriptions. Detailed 3-D structures of the spray can be analyzed from experimental data, by fixing different threshold values of μ_e as exemplified for the case of a GDI spray in Fig. 3. This type of data can be compared with simulated data by numerically deducing μ_e.

It should be emphasized that recent laser imaging techniques based on Structured Illumination are now capable of delivering this information even in optically dense situations. This gives to the modelers the possibility to verify if data generated by numerical simulations provides realistic 3-D spray structure, including the spray interior. Starting from this experimental/simulation comparison approach, improvements can be made to the simulations, and the model can, then, be further used to extract detailed information regarding droplet diameter distributions, liquid volume fractions, droplet number densities, etc. Nevertheless it should reminded that a complete model validation would require additional measurements such as the determination of droplet size as the extinction coefficient is related to two quantities (size and number density of droplets). By combining the measurement of both μ_e and droplets SMD using SLIPI-LIF/Mie droplets sizing calibrated with Phase Doppler (as recently shown in Mishra et al., 2014) the full characterization of the spray region could be experimentally reached. This future work would then provide the complete required experimental data in 3D for a proper model validation of the spray region.

Review of the techniques for the measurement of the local extinction coefficient

Multiple light scattering and Structured Illumination

The main challenge associated with optical diagnostics of spray systems is related to the multiple light scattering phenomenon, i.e. where photons interacts repeatedly with the liquid droplets. The detection of multiply scattered photons leads to image distortions in the form of image blur and limits quantitative measurements, such as the measurement of droplets size and of the extinction coefficient. However, even though the majority of photons are being multiply scattered within the spray, some "useful" photons remain. Having a filtering strategy which allows the detection of those desired photons only, is then necessary if one wants to obtain reliable measurements in atomizing sprays. Such filtering can be achieved by means of Structured Illumination. The technique is an efficient optical "sorting" method suppressing the multiply scattered light intensity while retaining the contribution from singly scattered photons in the case of side scattering detection and from the ballistic photons in the case of transmission detection.
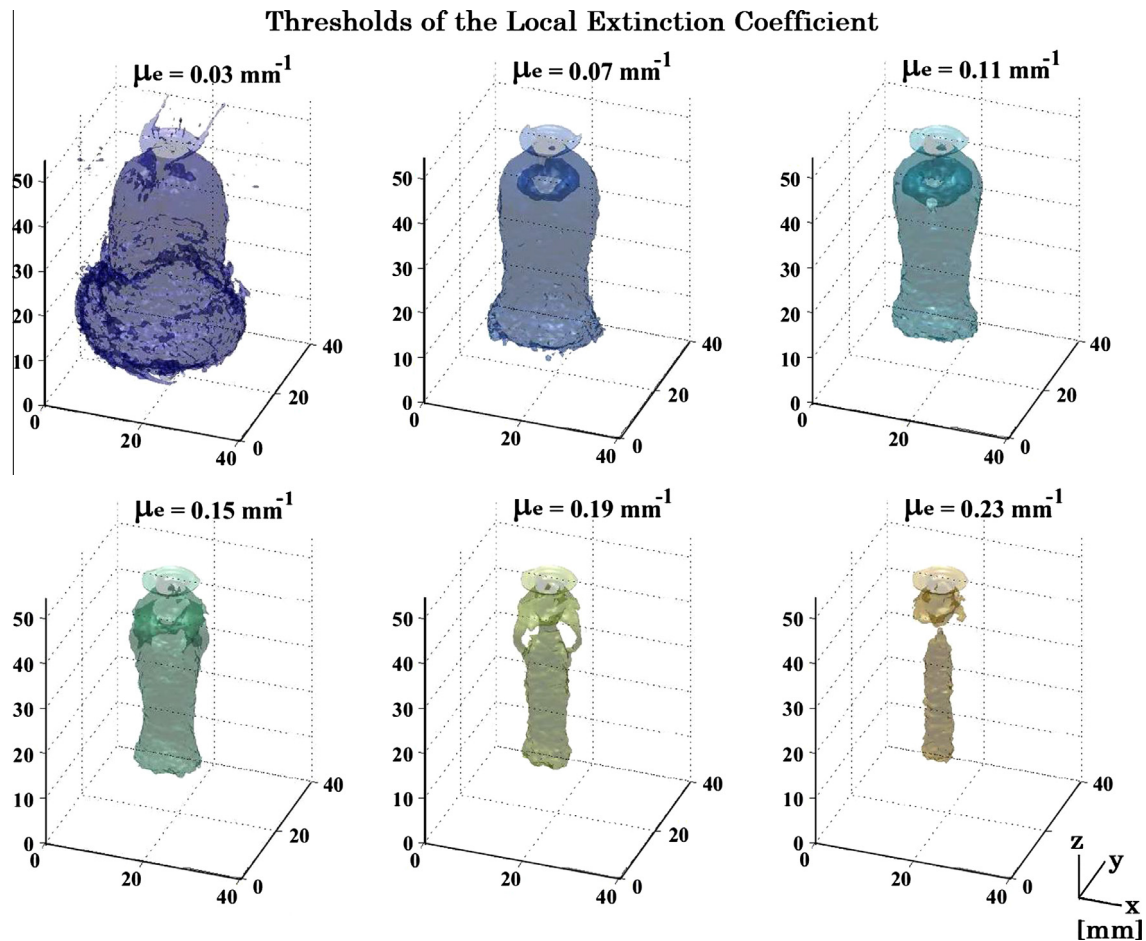
Thresholds of the Local Extinction Coefficient

Fig. 3. Determination of the 3D contours of a GDI spray for different values of the local extinction coefficient. Using this type of experimental data (published in Kristensson (2012) and Kristensson et al. (2012)) modelers can now compare the 3D shape of the spray for different threshold values of μ_e. It is seen that the spray penetration length differs as a function of the threshold value chosen. For experiment/simulation comparison purposes, one would need to make sure that the exact same threshold is applied on both data.

In Structured Illumination a recognizable pattern is added to the intensity profile of the light beam used to probe the sample of interest. Although most patterns will suffice, it is mathematically convenient to use a sinusoidal structure. The purpose of the pattern is that only singly scattered and unperturbed photons will maintain this structural information while propagating through the spray. On the opposite, multiply scattered photons will "forget" the superimposed structure.

With this feature, it becomes possible to reject the intensity contribution stemming from the multiply scattered light by post-processing the acquired data, thus allowing sprays with an *OD* exceeding unity to be investigated accurately. This concept was first demonstrated qualitatively by Berrocal et al. (2008) and Kristensson et al. (2008) in Berrocal et al. (2008), where laser sheet imaging was applied using a Structured Illumination scheme, a technique referred to as SLIPI (Structured Laser Illumination Planar Imaging). The technique is described in Fig. 4 where the modulated images are shown together with the SLIPI image. Since its creation in 2008, the authors have extended the technique to correct for effects of laser extinction and signal attenuation leading to the measurement of the local extinction coefficient in 2-D and 3-D.

Three-dimensional measurements: SLIPI-scan and Tomo-SLITI

The first approach to extract the local extinction coefficient in 3-D is called SLIPI-scan. As suggested by its name, the technique is based on a scanning procedure where successive 2-D sections of the spray are acquired sequentially. The key concept of the method is that it combines simultaneous transmission- and side-scattering detection, where the former provides information related to the overall reduction of light as it crosses the spray, while the latter reveals *where* the attenuation occurred. Combining the two information permits the user to calculate the local extinction coefficient of the spray. By collecting these data from several 2-D sections, a quantitative description of the spray can be constructed in 3-D. However, it is important to note that the scanning procedure must start at the very border of the spray, as the signal in each probed 2-D section must be compensated for the attenuation occurring in-between the light sheet and the camera. This requirement makes the approach relatively time-consuming to reach data from the spray center. Fig. 5(a) shows an example of a SLIPI-scan set-up. The spray system is mounted on a translational stage to enable the scanning and the dye-cuvette is used to visualize the transmitted light intensity. The accompanying result shows the 3-D structure of a solid cone water spray. The detailed description of the SLIPI-scan concept is given in Wellander et al. (2011).

The second approach to extract the local extinction coefficient in 3-D is called Tomo-SLITI which refers to the unification of tomographic reconstruction and transmission imaging using Structured Illumination (SLITI stands for Structured Laser Illumination Transmission Imaging). Tomography is a well-known method for reconstructions in 3-D, especially for medical applications, and is
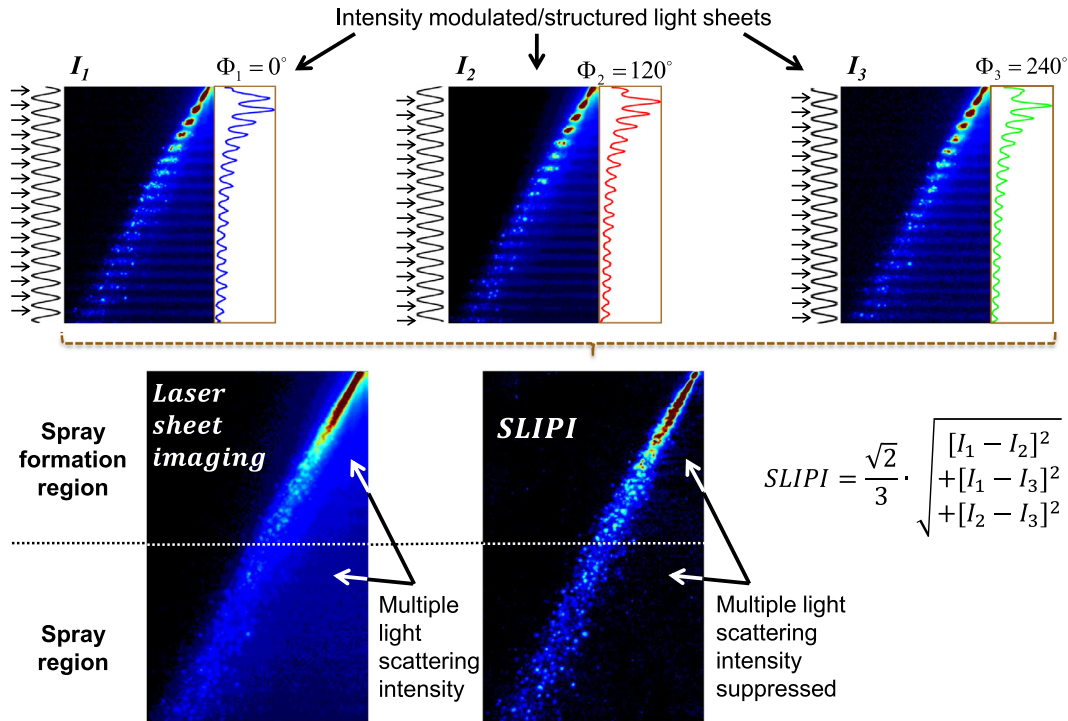
Fig. 4. Illustration of the SLIPI technique: Three successive images taken of a hollow-cone spray using a spatially modulated laser sheet. Each laser sheet illuminates the spray differently by changing the spatial phase Φ of the modulation. By averaging the sub-images, a conventional laser sheet image is obtained, in which the image is affected by multiple light scattering artifacts. By instead extracting the absolute value of the pairwise differences between the images (corresponding to the measurement of the modulation amplitude), the SLIPI image is formed. In this new image, the hollowness of the spray is clearly visible. The removed intensity corresponds to the contribution from multiple light scattering.

based on collecting an ensemble of transmission images, acquired from different viewing angles. Despite its merits, the approach has only been mildly applied for spray characterization due to limitations from multiple light scattering detection. However, by combining tomography and Structured Illumination, the unwanted contribution arising from multiply scattered photons can now be suppressed making it applicable for the study of optically dense sprays (up to $OD <\sim 6$). Fig. 5(b) shows an example of the Tomo-SLITI set-up. The structured laser light beam is guided through the spray and projected onto a screen. A camera collects this transmitted light with and without the spray running. The spray nozzle is mounted on a rotational stage to allow alterations to the viewing angle. The detailed description of Tomo-SLITI is given in Kristensson et al. (2012).

Two-dimensional measurements: Dual-SLIPI

Dual-SLIPI is a technique capable of directly extracting a 2-D mapping of the extinction coefficient without the need of a scanning or rotation procedures and of a heavy image post-processing. As a result, the approach presents the benefit of significantly reducing the total acquisition time. To gain access to the extinction of light, Dual-SLIPI aims at quantifying the reduction of the generated *signal* and not of the incident light sheet. This is achieved by performing two SLIPI measurements (hence the name) for two positions of the illumination planes and by recording the images with two cameras (one on either side of the spray).

Under the assumption that the Beer–Lambert law is valid, differences in intensity between these two acquisitions permits the user to calculate the extinction coefficient in the volume in-between the two laser sheet planes, thus generating a 2-D view of the *integrated* attenuation of light in this volume. Fig. 5(c) illustrates the detection arrangement associated with Dual-SLIPI. The spray is mounted on a translational stage for the required shift of

Δz and the cameras are aligned to have the same field-of-view. The detailed description of Dual-SLIPI is given in Kristensson et al. (2011).

A relevant advantage of Dual-SLIPI is that the technique can work based on a bi-directional illumination (or by rotating the spray 180°) allowing the measurement at twice the optical depth than SLIPI-scan and Tomo-SLITI. In addition, the technique can also be combined with either a scanning or a rotation procedure to generate 3-D data if required. However, one drawback of Dual-SLIPI is that two cameras and three optical accesses are required to operate it, while in SLIPI-Scan and Tomo-SLITI only one camera and two optical accesses are needed. In addition, the two cameras need to be carefully aligned to image exactly the same field with the same pixel resolution. Once recorded the images must then be warped to ensure a pixel-to-pixel overlapping of the image information.

Numerical calculation of the local light extinction coefficient

The process of deriving the light extinction coefficient numerically and comparing with experimental data is visualized in Fig. 7, and explained in detail in the following.

Determination of the extinction cross-sections

The calculation of the extinction coefficient μ_e from spray simulation results requires to determine, first, the extinction cross-section σ_e. The extinction cross-section corresponds to the total power scattered and absorbed by a particle divided by the incident density of the flux power that falls on it. As such, it is dependent on the incident wavelength, on the refractive indices of both the droplets and the surrounding medium and on the droplet diameter. The resulting σ_e surface can either be larger or smaller than the geometrical cross-section of the particle. In the case of spray
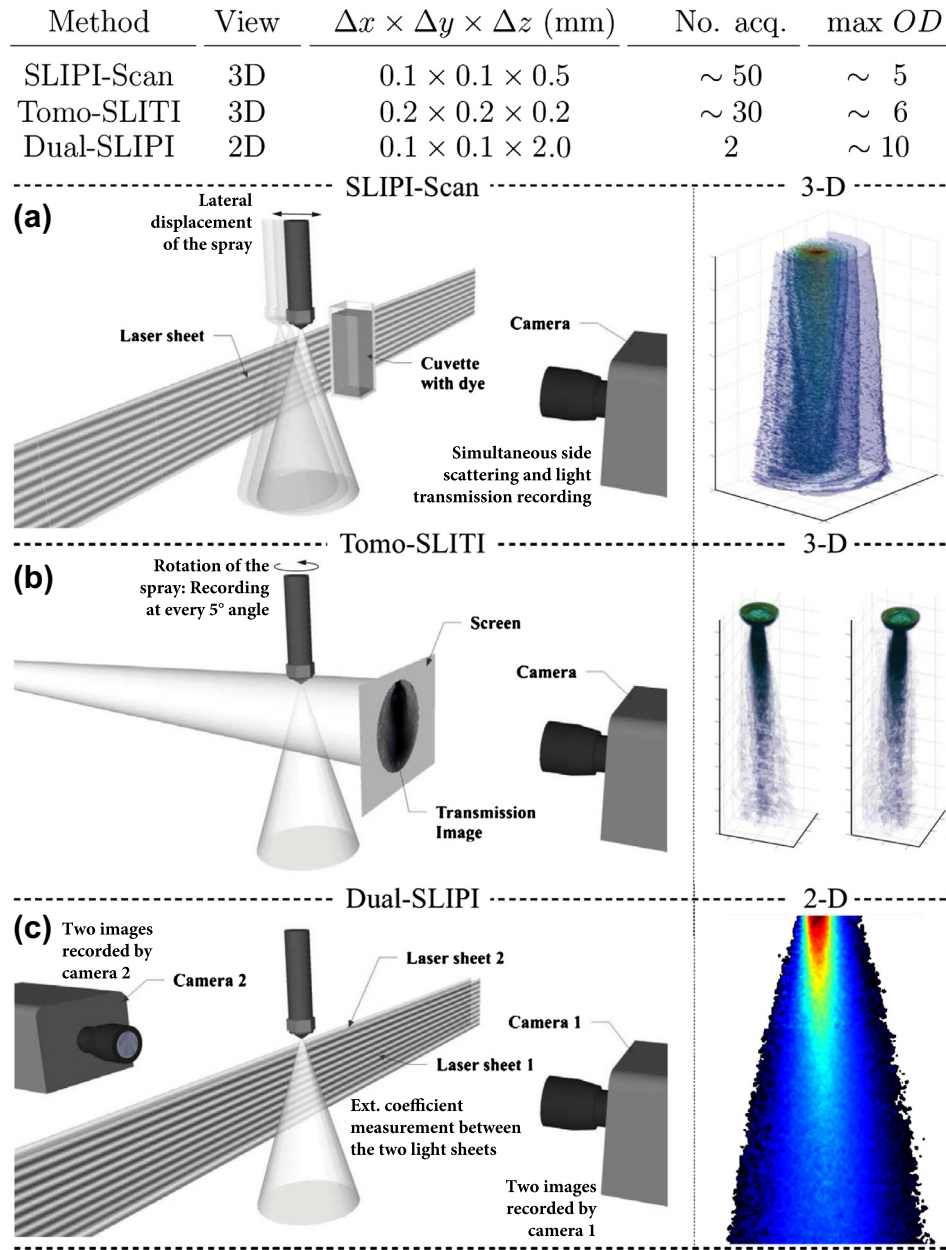
Method	View	$\Delta x \times \Delta y \times \Delta z$ (mm)	No. acq.	max OD
SLIPI-Scan	3D	$0.1 \times 0.1 \times 0.5$	~ 50	~ 5
Tomo-SLITI	3D	$0.2 \times 0.2 \times 0.2$	~ 30	~ 6
Dual-SLIPI	2D	$0.1 \times 0.1 \times 2.0$	2	~ 10

Fig. 5. Schematic and comparison of the experimental methods for (a) SLIPI-Scan, (b) Tomo-SLITI and (c) Dual-SLIPI. Each set-up is accompanied by an example result of a solid cone water spray. Note that all presented values in the table on the top of the figure are based on values from references Wellander et al. (2011), Kristensson et al. (2012, 2011). Those three techniques are the ones highlighted in blue in the table shown in Fig. 1. (For interpretation of the references to colour in this figure legend, the reader is referred to the web version of this article.)

systems consisting of spherical droplets in the range of tenth of microns and illuminated in the visible light spectrum, σ_e is $\approx$ twice as large as the geometrical cross-section σ_g of the droplets.

$$\sigma_e \approx 2 \cdot \sigma_g \approx \frac{\pi \cdot d_d^2}{2} \tag{4}$$

This approximation gives a rapid idea of the value of the extinction cross-section for spray droplets as shown in Fig. 6. However, for validating spray models, it is important to determine the exact extinction coefficient. In this case, one should consider the Lorenz-Mie theory which describes the interaction of an electromagnetic plane wave with a spherical droplet. There is a large body of literature regarding the development of the Lorenz-Mie theory (Bohren and Huffman, 1983, see for example).

The goal of this section is not to enter in detail into this topic, but rather to give the necessary tools to spray modelers to easily

extract σ_e as a function of droplets diameter. One reliable and open access software which computes the Lorenz-Mie theory is called *Mie Plot* (Laven, 2014). A convenient feature of the software is the generation of the extinction cross section as a function of the droplet diameter as exemplified in Fig. 6 for the case of water droplets.

The droplets located in the spray region are usually small with reduced velocities. Under such conditions the surface tension forces, which tend to give a spherical shape to the droplets, are dominant. As a results, the assumption of having spherical droplets in this region is most often valid and σ_e can be calculated using the Lorenz-Mie theory when illuminated with a laser beam (plane wave illumination).

The effect of different wavelengths on the value of the extinction cross section is shown in Fig. 6(a). The relative variations are noticeable especially in the case of small droplets as shown in
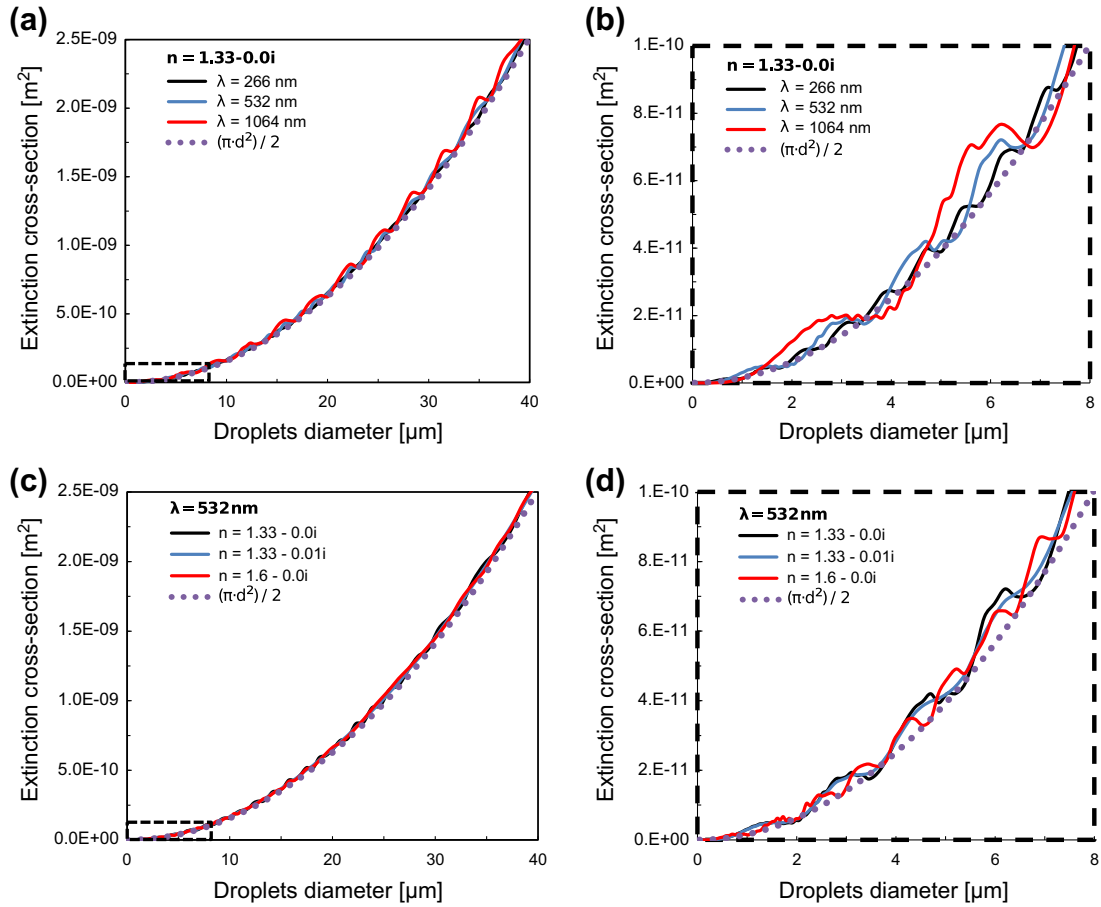
Fig. 6. (a): Relation between the extinction cross-section and the droplet diameter calculated from the Lorenz–Mie theory for three different illumination wavelengths, in the case of non-absorbing water droplets. A detailed view of (a) given in (b) for droplets smaller than 8 µm. (c): Relation between the extinction cross-section and the droplet diameter for three different refractive indices for an illumination wavelength fixed at 532 nm. A detailed view of (c) given in (d) for droplets smaller than 8 µm.

Fig. 7. Flowchart showing the process of deriving the local extinction coefficient using both the results of numerical simulations and input data from the experiment. The simulation gives the position vectors, $\mathbf{x}_m$, and diameters, $d_{d,m}$, of m droplets. The extinction cross-section for each droplet diameter, $\sigma_e(d_d)$, is derived from the Lorenz–Mie theory. By combining together this information with the knowledge of the experimental local volume, V_c, results of the simulated local extinction coefficients, $\mu_e(\mathbf{x})$, can be deduced and compared with the measured ones.

(b). Graph Fig. 6(c) is showing the effect of changes the in refractive index while keeping the illumination wavelength constant to 532 nm. Once again some fluctuations are observable especially for the small droplets as shown in (d). When absorption occurs in the droplets (e.g. the imaginary part of the droplets refractive index being above zero; here $n = 1.33 - 0.01i$), the fluctuations of the extinction cross-section are smoothed. The same effect is visible in Fig. 9 when $n = 1.40 - 0.1i$. This effect can be explained by the fact that the intensity of the refracted light is reduced due to absorption and does not interfere strongly anymore with the reflected light on the surface of the droplets. This results in a more smooth light intensity distribution of the scattered light intensity in the far field and in a more smooth value of the extinction cross-section.

Determination of the extinction coefficient within a local volume

Based on the knowledge of the extinction cross-section, this sub-section provides the procedure of how to derive the local light extinction coefficient, assuming the spatially resolved droplet size distribution is available from numerical simulation results. When assuming a uniform size of droplets the extinction coefficient is defined by Eq. (3). This assumption is valid for monodispersed systems but not in the case of spray systems where a droplet size distribution must be considered. In effect, atomizing sprays are characterized by a wide range of droplet sizes, not only globally but also locally. To each droplet size corresponds a given extinction cross-section. Thus, to obtain the local extinction coefficient, one needs to integrate the extinction cross-sections $\sigma_e(d_d)$ relating to the local droplet size distribution function.

Some numerical methods for dispersed two-phase flows, such as the Method-of-Moments (Hulburt and Katz, 1964) or the Quadrature Method-of-Moments (McGraw, 1997), both versions of the Two-fluid method, solve directly for the function of the local droplet size distribution, respectively the moments of the distribution. In this case, the local extinction coefficient at the position vector $\mathbf{x} = (x, y, z)$ can be derived directly by integration of the local droplet diameter distribution function, ψ, such as

$$\mu_e(\mathbf{x}) = \int_{d_d=0}^{d_{d,max}} \sigma_e(d_d) \cdot \psi(d_d, \mathbf{x}) \, dd_d. \tag{5}$$

However, if the LPT method or an interface resolving (such as VOF or level-set) is applied, individual droplets are tracked instead of continuous distribution functions. In this case the extinction cross-sections related to the droplets can be averaged over a local measurement volume, V_c, to obtain a local average of the extinction coefficient. If the number of droplets present in the measurement volume is n_d, the local extinction coefficient becomes

$$\mu_e(\mathbf{x}) = \frac{1}{V_c} \sum_{m=1}^{n_d(\mathbf{x})} \sigma_e(d_{d,m}). \tag{6}$$

If the stochastic parcel method is used (such as in the simulation presented herein, see Appendix A), where one computational parcel represents a number of φ droplets, then, for a measurement volume containing n_p parcels, the local extinction cross-section becomes

$$\mu_e(\mathbf{x}) = \frac{1}{V_c} \sum_{m=1}^{n_p(\mathbf{x})} \sigma_e(d_{d,m}) \cdot \varphi_m. \tag{7}$$

The accuracy of the estimated extinction coefficient depends on the accuracy of the extinction cross-section and on the determination of the local measurement volume. When comparing results between the simulated and experimental local extinction coefficient it is of utmost importance to define equivalent local volumes. Experimentally, the x and y dimensions of those volumes are defined by the pixel resolution of the recorded images, which is of the order of 100 μm if 10 cm of the spray region is imaged. The z dimension must be defined according to the experimental specifications which is related to the optical technique employed.

Example of comparison for a non-combusting Diesel spray

Description of the experiment

To show its potential the proposed method is applied for a non-combusting Diesel spray. The experimental results have been produced from a previous study which is detailed in Berrocal et al. (2012). The liquid, n-decane, is injected through a nozzle orifice of $d_{noz} = 105$ μm in diameter. The pressure inside the vessel is set to 18.6 bar while the rail pressure is 1100 bar. The temperature of the gas in the vessel is ambient, $\sim 20\,°C$. The n-decane liquid is injected during a period of $t = 1500$ μs and the Dual-SLIPI technique is used to image the spray at late time after injection start, corresponding to $t = 2000$ μs. In the first step of Dual-SLIPI, two SLIPI images are recorded by simultaneously imaging the laser sheet from both sides with two cameras. In the second step the laser sheet is displaced by a distance Δz within the spray and two more SLIPI images are extracted. Thus, four SLIPI images, $S_{P1,C1}, S_{P1,C2}, S_{P2,C1}$ and $S_{P2,C2}$ are created. P1 and P2 correspond to the two positions of the laser sheets, C1 and C2 correspond to the two cameras. The extinction coefficient can be directly determined from these four images, such as:

$$\mu_e = \ln\left(\frac{S_{P1,C1} \cdot S_{P2,C2}}{S_{P2,C1} \cdot S_{P1,C2}}\right) \cdot \frac{1}{2\Delta z}, \tag{8}$$

where Δz is the distance between the two laser sheets. In the current results, $\Delta z = 2$ mm. The SLIPI images are taken with two intensified CCD cameras of $1280 \cdot 1024$ pixels and with an image pixel resolution of $30\,μm \cdot 30\,μm$. The spray is illuminated at $\lambda = 355$ nm using the third harmonic of a pulsed (2–3 ns pulse width) Nd:YAG laser. The formed modulated light sheet is 27 mm height and with a spatial period of the modulation of 400 μm. The final extinction coefficient is extracted by averaging a total of 90 modulated single-shot images.

General description of the simulation

In this work, a Large-Eddy Simulation (LES) of the spray is performed. The continuous gas phase is described in Eulerian and the dispersed liquid phase in Lagrangian framework. This approach assumes the droplets to be small with relatively large inter-droplet distance and not interacting with each other, i.e. no collision or history/wake effects. The droplets are assumed to be spherical so they can be tracked individually and the subsequent breakup and momentum exchange processes can be modeled. As the LPT is a point-particle approach it assumes that the volume occupied by the liquid in each computational cell is small compared to the volume occupied by the gas (Sirignano, 1999, a detailed discussion concerning this topic can be found in chap. 8). All the above assumptions are often violated in spray simulations in a region very close to the injection nozzle. In the current simulations the liquid occupies in average less than 5% of the volume of a cell in a region beginning 15 nozzle diameters downstream. However, as the spray region is simulated here where the spray development occurs at more than 50 nozzle diameters from the orifice, the used methods are appropriate.

To account for secondary droplet breakup, in this work the approach of Caraeni et al. (2000) is followed: the two breakup regimes that are considered to be dominating are modeled, namely bag breakup and stripping breakup. The Wave Breakup model

Table 1
Initial conditions used in the simulation.

Parameter	Value
Liquid velocity	130 m/s
Liquid mass flow	0.5 g/s
Injection duration	1500 μs
Nozzle diameter	105 μm
Spray full angle	22°
Number of accumulations	90
Injected fuel	n-decane

according to Reitz and Diwakar (1986) is applied as long as the droplets contain more than 95% of the initially injected mass. The model describes both, the stripping breakup and the bag breakup regime. If the droplet has less than 95% of the injected mass the Taylor Analogy Breakup model according to O'Rourke and Amsden (1978) is applied. The model describes the bag breakup regime and uses the analogy between a distorted droplet and a spring-mass system. The evaporation of liquid mass is taken into account by an evaporation model, which assumes that the droplet is composed of a single-component and has a spherical shape with uniform properties as described in Amsden et al. (1989).

Input data and parameters used in the simulation

The computational domain used for the simulation is a cube with an edge length of 0.1 m. Grid refinements are used, the finest grid which is located where the spray develops has a cell size of $1.5 \cdot 10^{-3}$ m in all three directions. This leads to $2.2 \cdot 10^{6}$ grid cells. The diameter of the injection nozzle equals $d_{noz} = 105$ μm, the injected liquid is n-decane, corresponding to the experiment (Berrocal et al., 2012). The liquid velocity at the injection is unknown in the experiment. However, it is estimated from the pressure difference between the rail and the vessel (which is approximately 1080 bar) and accounting for in-nozzle losses to 130 m/s. The liquid mass flow is estimated analog to 0.5 g/s. These values are confirmed by Particle Image Velocimetry (PIV) measurements of spray experiments under similar conditions in Brands et al. (2010). A summary of the initial conditions used in the simulation is given in Table 1. A Rosin–Rammler droplet size distribution was assumed at the injection, based on the results from previous PDA measurements of the spray under similar conditions (Reddemann et al., 2010,). To analyze the influence of the SMD, three particle size distributions were considered

corresponding to SMD = 10.7 μm, 16.1 μm and 21.6 μm. Those distributions are given in Fig. 8.

It shall be reminded that the droplet distribution function at injection, called the "blob-injection model" (Reitz, 1976), does not aim to be physical and should not be seen as a description of the spray formation region. However it is a practical method to define the resultant droplet field of the spray region, where the basic assumptions of the LPT method are valid.

In this study, 90 simulations are performed from which an ensemble average is extracted, to meet the corresponding 90 single-shots from the experiment. To obtain different results for each individual simulation, the initial droplet sizes and their positions are determined using random numbers. The control volume used in the simulation must be identical to the control volume in the experimental setting. In the presented case, the volume V_c is chosen as a cuboid given as $V_c := \delta x \cdot \delta y \cdot \Delta z$. The image pixel resolution, 30 μm, corresponds to δx and δy and the distance between the two laser sheets, 2 mm, corresponds to Δz.

Results of the two-dimensional local extinction coefficient

As explained in Section 'Determination of the extinction cross-sections', it is necessary to find the relation between the droplet diameter and the extinction cross-section to be able to extract the simulated extinction coefficient. This requires the knowledge of the droplets refractive index during the experiment. As this information was unknown in the current experiment, a sensitivity study for three different refractive indices at $\lambda = 355$ nm is performed. The selected refractive indices are: one for a non-absorbing fuel of $n = 1.40 - 0.0i$, one for a highly absorbing fuel of $n = 1.40 - 0.1i$, and one for a non-absorbing fuel of $n = 1.45 - 0.0i$.

It is observed from Fig. 9 that the differences between the resulting extinction cross-sections are negligible if a range of droplets size between 0 and 40 μm is considered. Thus, the refractive index $n = 1.40 + 0.0i$, corresponding to non-absorbing droplets, is chosen here.

Fig. 10 shows a comparison of the extinction coefficient field between simulations with three different initial droplets distribution (shown in Fig. 8) and the experiment. The nozzle orifice is located at the bottom of the figure. In contrast to the simulation, the experimental result shows that the spray is still attached to the nozzle even at $t = 2000$ μs. An apparent explanation is that the nozzle does not close sharply and some liquid keeps being injected after $t = 1500$ μs. On the contrary, in the numerical simulation it is assumed that the nozzle is perfectly closing at end of the injection. In this case, the entire droplet field has moved ~ 10 mm
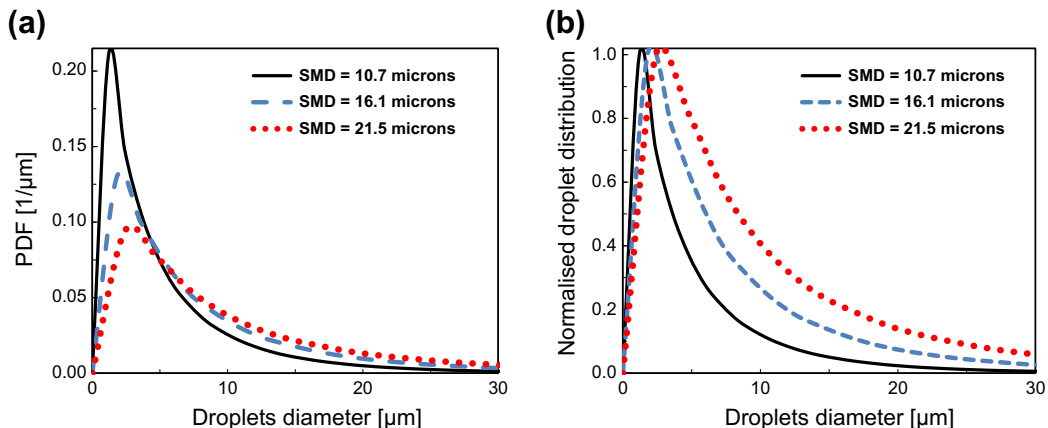

Fig. 8. Initial droplet diameter distributions used in the simulations, where the Probability Density Function (PDF) and the normalized distributions are given in (a) and (b) respectively. Three Rossin–Rammler distributions are considered, corresponding to SMD = 10.7 μm, 16.1 μm and 21.6 μm.
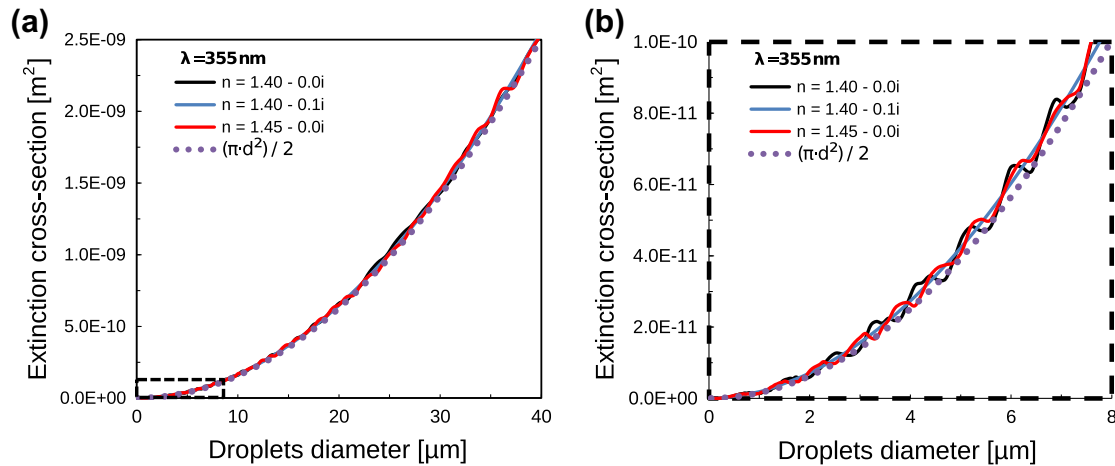
Fig. 9. Relation between the extinction cross-section and the droplet diameter for three different refractive indices at $\lambda = 355$ nm. Small changes of the refractive index induce small changes in the extinction cross-section.

downstream during the 500 μs separation time. Thus, the spray is no longer attached to the nozzle on the simulated results.

Due to the challenging spray conditions, Phase Doppler data is not available inside the droplets field. As a result, three different droplet diameter distributions were tested, assuming Rossin–Rammler distributions, where a SMD of 10.7 μm, 16.1 μm and 21.5 μm was used as input data respectively. In all cases, the same amount of liquid fuel was injected and the number of droplets was deduced accordingly. It is seen from these results that smaller initial droplets sizes, with SMD = 10.7 μm, lead to an over-prediction of the experimental extinction coefficient by a factor of ~two. On the contrary, larger initial droplet sizes with SMD = 21.5 μm lead to an underprediction of the extinction coefficient. Finally, when using an initial droplet size distribution with SMD = 16.1 μm similar values of μ_e are found between the experimental and simulated results. This is observed for both the inside and the periphery of the spray. This observation demonstrates the importance in fixing an accurate initial droplet size distribution in the numerical simulations.

It can be seen that the experimental data are not accessible on the left side of the spray (shown in the grey area). This is due to the strong reduction of the Signal-to-Noise Ratio (SNR) induced by light extinction as the laser sheet crosses the spray (here from the right side of the image to the left). These effects are more or less important depending on the optical density of the probed spray. It can, however, be compensated by using counter propagating light sheets or by rotating the spray nozzle.

In the computed results large ring-like structures can be observed at 18 mm axial position. The lack of these structures in the experimental data suggests that these features are probably generated through the simulation by large-scale coherent structures as a result of entrainment and vortex shedding at the shear layers of the jet. In the experiments the surrounding air, in the beginning of each injection, is not perfectly quiescent, influencing the evolution of the large-scale structures which might follow different paths and/or break down earlier. As a result of averaging over a large number of injection events the effect of the large scale structures is smoothed out, explaining why those structures are not visible experimentally.

When analyzing these results, one should keep in mind that the extinction coefficient field represents a combination of a droplet number density and the related droplet extinction cross-sections. Thus, a certain extinction coefficient field can either be obtained from many small droplets or from fewer larger droplets.

Nevertheless, comparing experimental and numerical extinction coefficient fields gives a strong initial indication that the simulation reflects faithfully or not the spray structure observed experimentally.
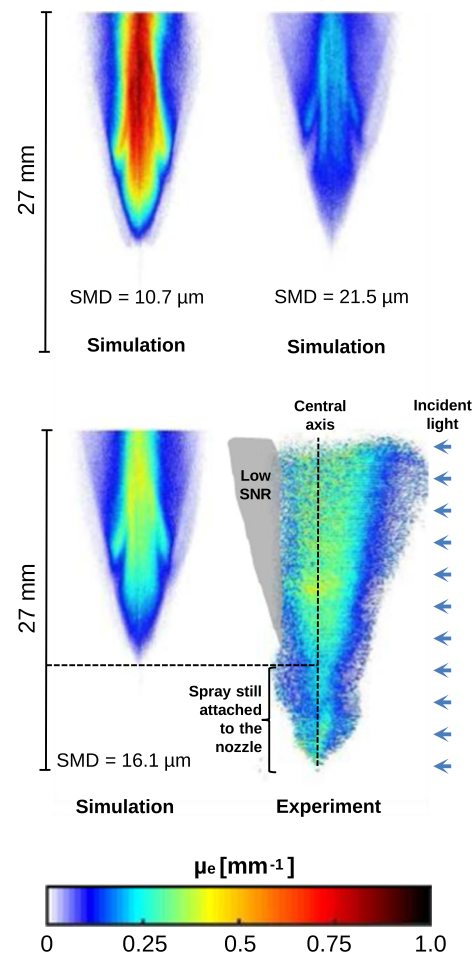

Fig. 10. Comparison between simulated and experimental results for the local ensemble averaged extinction coefficient. The LPT simulations results for SMD = 10.7 μm, 16.1 μm and 21.5 μm are shown together with the Dual-SLIPI experimental results. All cases correspond to $t = 2000$ μs after injection start, while the closing of the needle was fixed to $t = 1500$ μs.
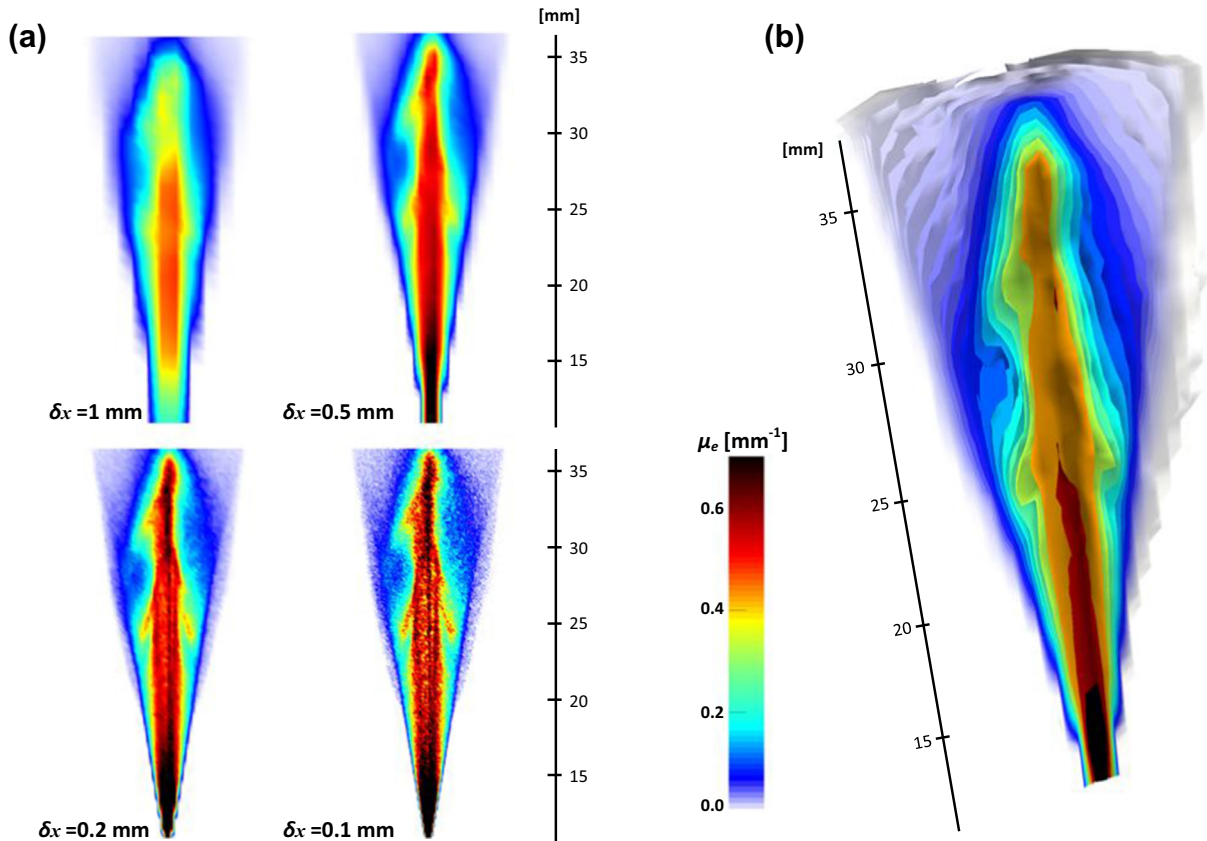
Fig. 11. Numerically computed extinction coefficient at $t = 1500$ μs with SMD = 16.1 μm . (a) 2-D visualisation for decreasing control volume sizes from 1 to 0.1 mm. (b) 3-D iso surfaces of the extinction coefficient in the case of 0.5 mm volumes.

Further results from the numerical simulations

Three-dimensional extinction coefficient: effects of the size of the local volumes

The local light extinction coefficient obtained experimentally is averaged both spatially and over a number of injections. To provide comparable data the numerical results must undergo the same averaging procedures. Therefore, the results from 90 simulations were ensemble averaged to match the 90 injections considered experimentally. Regarding the spatial averaging, the averaged local extinction coefficient is deduced over the chosen local measurement volume V_c. In the previous section the volume used in the numerical simulation was identical in size and shape to the volume used in the Dual-SLIPI experiment. Changing the size of V_c leads to different results of μ_e. The size of the local volumes should be large enough to contain a statistically representation of the droplets number density, but small enough to maintain a good spatial resolution.

Fig. 11(a) shows the effect of resolution on the local light extinction coefficient for different sizes of local measurement volumes for the case of SMD = 16.1 μm . A cubical shape of the local volumes is chosen here in order to have the same resolution in all three directions. By comparing the extinction coefficient plots obtained with different resolutions, averaging effects for large measurement volume sizes (1 mm) can be observed. However, also for $\delta x \leqslant 1$ mm the predicted values are in the same order of magnitude, except close to the nozzle. In this region applicability of both the optical experimental methods and the chosen numerical method (LPT) are anyhow limited due the large droplet density. Further downstream however, the decreasing control volume size

increases as expected the amount of details captured. The finest resolution case ($\delta x = 0.1$ mm) has qualitatively and quantitatively the same information like the case with $\delta x = 0.2$ mm, however, more noise can be seen indicating the lower resolution for this dataset. Using more samples in the averaging procedure will reduce this noise.

An example of 3-D numerical data is shown in Fig. 11(b), where the 3-D isosurfaces of the local extinction coefficient are shown. As expected, an increased value of the extinction coefficient close to the spray center is observed, due to large droplet concentrations.

Two-dimensional optical depth

The optical depth is another optical parameter that can be analyzed. It can be deduced by multiplying the extinction coefficient μ_e with the distance x crossed by a beam of light as shown in Eq. (2). The *OD* can is an approximation of the average number of scattering events experienced by a photon packet when traveling through the spray. Fig. 12 shows the values of the optical depth at various time instances after injection start.

The simulations with initial SMD = 10.7 μm and with SMD = 16.1 μm are shown in (a) and (b). It is seen that an increase of 5 μm in droplet SMD results in a reduction of the *OD* by a factor of two. From this observation it is deduced that LPT simulations with too large or too small droplet size distributions as initial condition leads to non-realistic spray systems. In the first case the spray will be much more optically dilute while in the second case it will be much more optically dense than it is in the reality.

In the present case, the maximum value of the optical depth is reaching 5 for SMD = 10.7 μm and 2.5 only with SMD = 16.1 μm. Based on previous light transmission experimental results (Payri

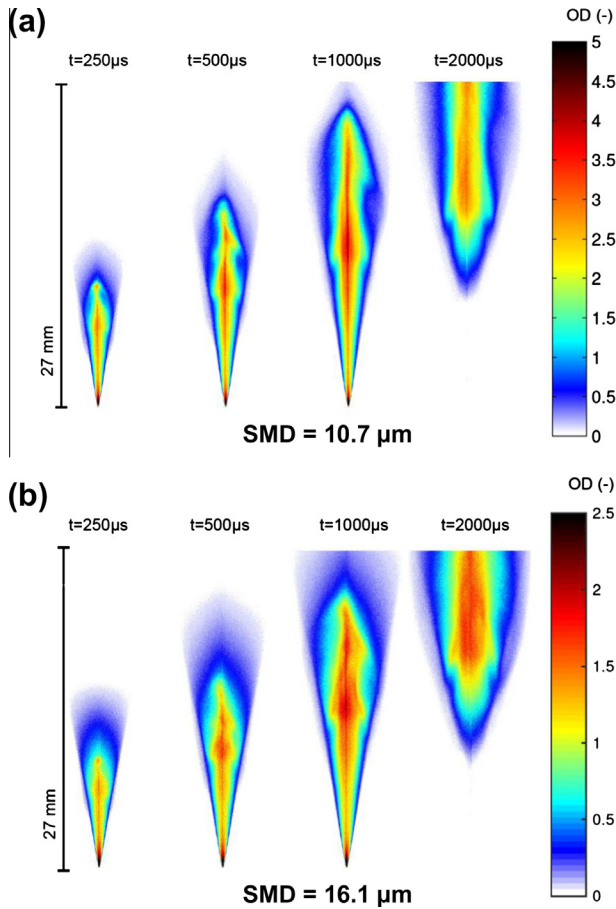**Fig. 12.** Numerically computed optical depth fields for $t = 250, 500, 1000$ and 2000 μs (from left to right). In (a), the SMD = 10.7 μm and in (b) the SMD = 16.1 μm. It is seen that the resulting optical depth is particularly sensitive to the initial droplet size distribution used in the model.

et al., 2011), the *OD* is found to be superior to 5 in the case of Diesel spray, supporting the use of SMD = 10.7 μm. However, Fig. 10 shows that the values of the extinction coefficient agrees better at SMD = 16.1 μm. At the same time, Fig. 10 also shows that the experimental spray, at $t = 2000$ μs after injection start, is twice as large than the simulated one, confirming a larger *OD* in the experimental results. It is then deduced that the droplets transport and spreading in space is different between the experiment and the simulation. All those observations from experiment/simulation comparison highlights the importance in combining the knowledge of the local extinction coefficient and of the *OD*, if one wants to gain more accurate guidance for improving the modeling approach.

Summary and conclusions

In optically dense situation, where Phase Doppler data cannot be extracted, the attempts of spray model validation have been mostly based on the correlation of global parameters, such as the spray penetration length (from shadowgraph images), the vapor penetration distance (from schlieren images) and the spray opening angle. However, those parameters do not describe the intrinsic properties of the droplet fields, which includes the size and concentration of droplets. In addition, they are most often integrated along a line-of-sight and lack high spatial resolution.

In this article three advanced laser imaging techniques based on Structured Illumination have been presented as a solution to

provide quantitative spray information in 2-D and 3-D, even in optically dense situations. The extracted experimental data corresponds to the extinction coefficient field which is a faithful quantity for the description of the spray region and can be used for experiment/simulation results comparisons.

The numerical procedure to reach this goal has been proposed and described in a general form in order to be applied for a wide range of modeling techniques (such as Two-fluid, LPT and interface resolving methods, such as VOF or level-set). An example of the proposed method has been shown for the spray region of a non-combusting Diesel spray. The local extinction coefficient field was obtained experimentally using the Dual-SLIPI technique and numerically using the LPT method.

The comparison between experimental and simulated results have demonstrated the important advantage of the proposed method: Instead of considering global parameters, spatially and temporally resolved data have been compared. This gives the possibility to clearly identify in which regions the spray is adequately modeled and in which it is not, allowing the modelers to draw conclusions about the sources of the modeling error, which is hardly possible with the previous comparison approaches.

Acknowledgements

Appendix A. Continuous phase in the numerical simulation

The continuous gaseous phase is described in the Eulerian framework by the continuity and momentum transport equations for incompressible, Newtonian fluids with constant diffusivities, given in Eqs. (A.1), and (A.2). Due to the assumption of a large inter-droplet distance spray, the continuous phase volume fraction is assumed to be unity.

$$\frac{\partial \rho_g}{\partial t} + \frac{\partial \rho_g u_j}{\partial x_j} = 0 \tag{A.1}$$

$$\frac{\partial \rho_g u_i}{\partial t} + \frac{\partial \rho_g u_i u_j}{\partial x_j} = -\frac{\partial p}{\partial x_i} + \frac{\partial}{\partial x_j} \mu_g \frac{\partial u_i}{\partial x_j} + \dot{F}_{S,i} \tag{A.2}$$

$\dot{F}_{S,i}$ is the source term which accounts for the momentum coupling between the liquid to the gaseous phase. u, ρ_g, μ_g and p denote the gas velocity, density, dynamic viscosity and pressure, respectively.

The governing equations are discretized by the Finite-Difference-Method (FDM). The convective terms are approximated by an up to fifth-order Weighted Essentially Non Oscillatory (WENO) scheme, which was developed by Jang and Shu (1996). The pressure terms and the diffusive terms are approximated by fourth-order central scheme and the time derivatives are approximated by an implicit second-order backward scheme. For grid points close to the boundary of the domain, lower order approximations are used. The resulting system of equations is solved applying the Semi-Implicit Method for Pressure Linked Equations (SIMPLE) algorithm, according to Caretto et al. (1972) and Patankar (1975).

When Eqs. (A.1) and (A.2) are solved several numerical errors are introduced, out of which the spatial truncation error is the largest. This error has a form of a numerical stress and is depending on the cell size. In this work no explicit turbulence model is used, but the truncation error is assumed to be of the same magnitude as the residual stresses. As both, the residual and the numerical stresses depend on the cell size (as the numerical grid acts as spatial

filter), this assumption is true for small cells. The filtering and residual stress modeling is done implicitly by the numerical schemes. This approach has been applied successfully in previous works under similar conditions i.e. LPT spray simulations (Salewski et al., 2008; Salewski and Duwig, 2007; Iudiciani and Duwig, 2009).

Appendix B. Dispersed phase in the numerical simulation

The droplet distribution function is given by

$$f(\vec{x}, \vec{u}_d, d_d, T_d, y, \dot{y})d\vec{x}\,d\vec{u}_d\,dd_d\,dT_d\,dy\,d\dot{y} \qquad (B.1)$$

This function gives the number of droplets that are currently at a position between $\vec{x}$ and $\vec{x} + d\vec{x}$, of a speed between $\vec{u}_d$ and $\vec{u}_d + d\vec{u}_d$, of a diameter between d_d and $d_d + dd_d$, of a temperature between T_d and $T_d + dT_d$ and of distortion parameters between y and $y + dy$ and the distortion rates $\dot{y}$ and $\dot{y} + d\dot{y}$. The liquid phase is described by the stochastic parcel method, which is a discrete representation of the continuous droplet distribution function. The total number of droplets is gathered in parcels each representing the corresponding number of droplets, f. Each parcel is considered as a particle and tracked individually in the Lagrangian Particle Tracking framework.

Only aerodynamic drag forces are taken into account for the momentum exchange between gaseous and liquid phases. The acceleration of a spherical, isolated, rigid droplet is according to Newton's second law of motion,

$$\frac{d\vec{u}_d}{dt} = -\frac{3\rho_g}{4\rho_l d_d}C_d\,|\vec{u}_{rel}|\,\vec{u}_{rel}, \qquad (B.2)$$

where C_d is the drag coefficient of the droplet. C_d is depending on the droplet Reynolds number and follows the standard drag curve for a smooth sphere Schiller and Neumann (1933). There are other forces acting on the droplet such as the virtual mass force, the Faxen force, the Basset history term, gravitational forces, the Magnus force and the Saffman forces. These are neglected in the current work, as well as in most other similar spray simulations, which is justified in Salewski (2006) for similar spray conditions.

References

Amsden, A., O'Rourke, P., Butler, T., 1989. KIVA-II: A Computer Program for Chemically Reactive Flows with Sprays. Los Alamos National Laboratory (Tech. Rep. LA-11560-MS).

Andreassi, L., Ubertini, S., Alloca, L., 2007. Experimental and numerical analysis of high pressure diesel spray-wall interaction. Int. J. Multiphase Flow 33, 742–765.

Apte, S., Gorokhovski, M., Moin, P., 2003. LES of atomizing spray with stochastic modeling of secondary breakup. Int. J. Multiphase Flow 29, 1503–1522.

Balachandar, S., Eaton, J., 2010. Turbulent dispersed multiphase flow. Annu. Rev. Fluid Mech. 42, 111–133.

Beck, J., Watkins, A., 2002. On the development of spray submodels based on droplet size moments. J. Comput. Phys. 182, 586–621.

Berrocal, E., Kristensson, E., Hottenbach, P., Alden, M., Gruenefeld, G., 2012. Quantitative imaging of a non-combusting Diesel spray using Structured Laser Illumination Planar Imaging. Appl. Phys. B, Lasers Opt.

Berrocal, E., Kristensson, E., Richter, M., 2008. Application of structured illumination for multiple scattering suppression in planar laser imaging of dense sprays. Opt. Express 16, 17870–17881.

Bohren, C., Huffman, D., 1983. Absorption and Scattering of Light by Small Particles. Wiley, N.Y..

Brands, T., Hottenbach, P., Ko, H., Gruenefeld, G., Pichinger, S., Adomeit, P., 2010. Effects of ambient conditions and nozzle design on the velocity of clustered diesel jets. In: 15th Int. Symp. on Applications of Laser Techniques to Fluid Mechanics, Lisbon, Portugal.

Broukal, J., Hajek, J., 2011. Validation of an effervescent spray model with secondary atomization and its application to spray modeling of a large-scale furnace. Appl. Therm. Eng. 31, 2153–2164.

Caraeni, D., Bergström, C., Fuchs, L., 2000. Modeling of liquid fuel injection, evaporation and mixing in a gas turbine burner using large eddy simulation. Flow, Turbulence Combust. 65, 223–244.

Cardenes, M., Martin, D., Kneer, R., 2010. Experimental investigation of droplet size and velocity in clustered diesel sprays under high-pressure and high-temperature conditions. SAE Int. 10FFL-0076.

Caretto, L., Gosman, A., Patankar, S., Spalding, D., 1972. Two calculation procedures for steady, three-dimensional flows with recirculation. In: 3rd International Conference on Numerical Methods in Fluid Mechanics. II.

Crua, C., de Sercey, G., Heikal, M., Gold, M., 2012. Dropsizing of near-nozzle diesel and RME sprays by microscopic imaging. In: 12th Triennial International Conference on Liquid Atomization and Spray Systems (ICLASS), 2–6 September 2012, Heidelberg, Germany. <http://www.springerlink.com/index/10.1007/s002160050165>.

Desjardins, O., Moureau, V., Pitsch, H., 2008. An accurate conservative level set/ghost fluid method for simulating turbulent atomization. J. Comput. Phys. 227, 8395–8416.

Dukowicz, J.K., 1980. A particle-fluid numerical model for liquid sprays. J. Comput. Phys. 35, 229–253.

Faeth, G., Hsiang, L.-P., Wu, P., 1995. Structure and breakup properties of Sprays. Int. J. Multiphase Flow 21, 99–127.

Fu-shui, L., Lei, Z., Bai-gang, S., Zhi-jie, L., Schock, H., 2008. Validation and modification of WAVE spray model for diesel combustion simulation. Fuel 87, 3420–3427.

Hulburt, H., Katz, S., 1964. Some problems in particle technology: a statistical mechanical formulation. Chem. Eng. Sci. 19, 555–574, http://www.sciencedirect.com/science/article/pii/0009250964850478.

Iudiciani, P., Duwig, C., 2009. Large Eddy Simulation of the sensitivity of vortex breakdown and ame stabilization to axial forcing. Turbulence, Heat Mass Transfer.

Jang, G., Shu, C., 1996. Efficient implementation of weighted ENO schemes. J. Comput. Phys. 126, 202–228.

Kristensson, E., 2012. Structured Laser Illumination Planar Imaging, SLIPI, Applications for Spray Diagnostics. PhD Thesis.

Kristensson, E., Berrocal, E., Alden, M., 2011. Extinction coefficient imaging of turbid media using dual structured laser illumination planar imaging. Opt. Lett. 36, 1656–1658.

Kristensson, E., Berrocal, E., Aldén, M., 2012. Quantitative 3D imaging of scattering media using structured illumination and computed tomography. Opt. Express 20, 14437–14450, http://www.opticsexpress.org/abstract.cfm?URI=oe-20-13-14437.

Kristensson, E., Berrocal, E., Aldén, M., 2014. Two-pulse structured illumination imaging. Opt. Lett. 39, 2584–2587, http://ol.osa.org/abstract.cfm?URI=ol-39-9-2584.

Kristensson, E., Berrocal, E., Richter, M., Pettersson, S.-G., Aldén, M., 2008. High-speed structured planar laser illumination for contrast improvement of two-phase flow images. Opt. Lett. 33, 2752–2754, http://ol.osa.org/abstract.cfm?URI=ol-33-23-2752.

Kristensson, E., Richter, M., Alden, M., 2010. Nanosecond Structured Laser Illumination planar imaging for single-shot imaging of dense sprays. Atomizat. Sprays 20, 337–343.

Laven, P., 2014. MiePlot v. 4.3 – A Computer Program for Scattering of Light from a Sphere Using Mie Theory & the Debye Series. <http://www.philiplaven.com/mieplot.htm>.

Linne, M., 2013. Imaging in the optically dense regions of a spray: a review of developing techniques. Prog. Energy Combust. Sci. 39, 403–440, http://www.sciencedirect.com/science/article/pii/S0360128513000282.

Linne, M., Paciaroni, M., Berrocal, E., Sedarsky, D., 2009. Ballistic imaging of liquid breakup processes in dense sprays. Proc. Combust. Inst. 32, 2147–2161.

Loth, E., 2000. Numerical approaches for motion of dispersed particles, droplets and bubbles. Prog. Energy Combust. Sci 26, 161–223.

Martínez-Martínez, S., Sánchez-Cruz, F., Riesco-Ávila, J., Gallegos-Muñoz, A., Aceves, S., 2008. Liquid penetration length in direct diesel fuel injection. Appl. Therm. Eng. 28, 1756–1762, http://www.sciencedirect.com/science/article/pii/S1359431107003845.

McGraw, R., 1997. Description of aerosol dynamics by the quadrature method of moments. Aerosol Sci. Technol. 27, 255–265. http://dx.doi.org/10.1080/02786829708965471.

Menard, T., Tanguy, S., Berlemont, A., 2006. Coupling level set/VOF/ghost fluid methods: validation and application to 3D simulation of the primary break-up of a liquid jet. Int. J. Multiphase Flow 33, 510–524.

Mishra, Y.N., Kristensson, E., Berrocal, E., 2014. Reliable lif/mie droplet sizing in sprays using structured laser illumination planar imaging. Opt. Express 22, 4480–4492, http://www.opticsexpress.org/abstract.cfm?URI=oe-22-4-4480.

Naber, J.D., Siebers, D.L., 1996. Effects of gas density and vaporization on penetration and dispersion of diesel sprays. SAE Int. 96. http://dx.doi.org/10.4271/960034.

O'Rourke, P., Amsden, A., 1978. The TAB Model for Numerical Calculation of Spray Breakup. SAE Tech. Pap. 872089.

Patankar, S., 1975. Numerical prediction of three-dimensional flows. Studies Convect.: Theory, Measure. Appl. 1, 1–78.

Payri, F., Pastor, J., Payri, R., Manin, J., 2011. Determination of the optical depth of a DI diesel spray. J. Mech. Sci. Technol. 25, 209–219.

Picket, L., Genzale, C., Manin, J., Malbec, L.-M., Hermant, L., 2011. Measurement Uncertainty of liquid penetration in evaporating diesel sprays. In: ILASS Americas, 23rd Annual Conference on Liquid Atomization and Spray Systems, Ventura, CA.

Reddemann, M., Mathieu, F., Martin, D., Kneer, R., 2010. The influence of fuel properties on spray propagation, atomization and evaporation. In: ILASS – Europe 2010, 23rd Annual Conference on Liquid Atomization and Spray Systems, Brno, Czech Republic.

Reitz, R., 1976. Modeling atomization processes in high-pressure vaporizing sprays. Atomizat. Spray Technol. 3, 309–337.

Reitz, R., Diwakar, R., 1986. Effect of drop breakup on fuel sprays. SAE Tech. Pap. 860469.

Salewski, M., 2006. LES of Jets and Sprays injected into Crossflow. Ph.D. thesis, Lund University of Technology.

Salewski, M., Duwig, C., 2007. Large eddy simulation of spray combustion in a swirl-stabilized gas turbine burner. AIAA Paper 2007–5634.

Salewski, M., Stankovic, D., Fuchs, L., 2008. Mixing in circular and non-circular jets in crossflow. Flow, Turbulence Combust. v 80, 255–283.

Schiller, L., Neumann, A., 1933. A drag coefficient correlation. Z. Ver. Dtsch. Ing. 77, 318–320.

Shim, Y.-S., Choi, G.-J., Kim, D.-J., 2009. Numerical and experimental study on effect of wall geometry on wall impingement process of hollow-cone fuel spray under various ambient conditions. Int. J. Multiphase Flow 35, 885–895.

Shinjo, J., Umemura, A., 2011. Surface instability and primary atomization characteristics of straight liquid jet sprays. Int. J. Multiphase Flow 37, 1294–1304.

Sirignano, W.A., 1999. Fluid Dynamics and Transport of Droplets and Sprays. Cambridge University Press, Cambridge.

van Wachem, B., Almstedt, A., 2003. Methods for multiphase computational fluid dynamics. Chem. Eng. J. 96, 81–98.

Wellander, R., Berrocal, E., Kristensson, E., Richter, M., Alden, M., 2011. Three-dimensional measurement of the local extinction coeffcient in a dense spray. Meas. Sci. Technol., 22

Wu, Z., Zhu, Z., Huang, Z., 2006. An experimental study on the spray structure of oxygenated fuel using laser-based visualization and particle image velocimetry. Fuel 85, 1458–1464.